Voltage-Dependent Scanning Tunneling Microscopy Images of a Copper Complex on Graphite

Zhigang Wang,*,†,§ Qingdao Zeng,† Yanbing Luan,‖ Xiaojun Wu,‡ Lijun Wan,† Chen Wang,† Gil U Lee,§ Shuxia Yin,† Jinlong Yang,‡ and Chunli Bai*,†

The Center for Molecular Sciences, Institute of Chemistry, Chinese Academy of Sciences, Beijing, 100080, P. R. China, Lab of Bond Selective Chemistry, University of Science and Technology of China, Hefei, Anhui, 230026, P. R. China, School of Chemical Engineering, Purdue University, West Lafayette, Indiana 47907, and School of Materials Engineering, Purdue University, West Lafayette, Indiana 47907

Received: February 16, 2003; In Final Form: September 7, 2003

Dramatic contrast variation of STM images has been investigated as a function of bias on a bis[1,3-di(*p*-*n*-tetradecyloxyphenyl)propane-1,3-dionato] copper(II) (abbreviated as $C_{14}O-Cu$) adlayer physisorbed on HOPG with STM. It was found that STM images changed with bias change of 100 mV or less. Submolecular features of the molecular core and interdigitated alkyl chain were clearly revealed. A preliminary theoretical calculation was carried out to simulate the image variation. The simulated results were in agreement with STM observation.

Introduction

Scanning tunneling microscopy (STM) has emerged as a powerful tool used to investigate molecules adsorbed on conductive solid substrates with atomic resolution. STM images of molecules often strikingly match the chemist's intuition, but exactly how molecules are imaged is not obvious. Adsorbed molecules alter surface electronic structure, produce complex coupling between tip and substrate, and can be directly involved in resonant tunneling. Theoretically, the fundamentals of tunneling are well established and many computational approaches have been developed.[1−3] Detailed calculations of STM imaging have often been done for atoms on the surface, but molecular adsorbates greatly increase the complexity and cost of computation. There is a need for systematic experimental results on well-characterized systems to which theory can be compared.[4]

For molecular adsorbates, the contrast of the STM images corresponds to the density of states near the Fermi level arising from hybridization of the substrate states with the states in the molecules.[5−7] STM is working on the principle of electron tunneling between an atomically sharp tip and a sample surface,[7] detecting the electronic structure of the surface at the Fermi level. Images are usually obtained in two models of (1) the constant current, and (2) the constant height mode by scanning the tip laterally over the surface. The tunneling current (I_t) is in direct proportion to bias voltage by the relation of $I = (2\pi/\hbar)eV^2\sum_{\mu,\nu}|M_{\mu\nu}|^2\delta(E_\nu - E_F)\delta(E_\mu - E_F)$.[8] The variation of tunnel current is a function of bias voltage.

The previous studies presented experiment observations on dramatic voltage-dependent variations in the images of organic molecules chemisorbed on silicon.[4] Bias-induced changes of the internal contrast of a molecule adsorbate have been reported in the case of Cu−phthalocyanine[9] and copper(II) octaalkoxyl-substituted phthalocyanine,[10] and the internal contrast observed at positive sample bias is different from that at negative sample bias. The other papers[6,11−16] also presented interesting bias-dependent behaviors in the images of adsorbate.

SCHEME 1. Molecular Structure of C_nO-Cu

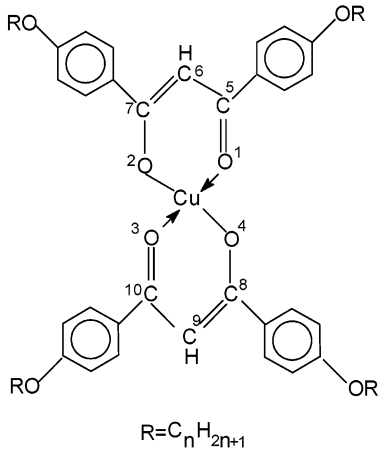

Highly oriented pyrolytic graphite (HOPG) is selected as a substrate for the study of adsorption of molecules on surfaces because of its relatively weak interaction with adsorbate and its easy cleavage resulting in large flat terraces.[17] It has long been demonstrated that organic molecules with long alkyl chains can be immobilized on the basal plane of HOPG.[18−23]

Herein we present systematically experimental observations of dramatic voltage-dependent contrast variations in images of $C_{14}O-Cu$ physisorbed on HOPG. The molecule consists of a core and alkane chains. The molecular structure is shown in Scheme 1. In the core, four oxygen atoms surround a copper atom. An inert HOPG was used as substrate for molecule adsorption. The large-sized molecule was deposited on the HOPG surface. STM imaging revealed the adlayer structure and molecular arrangement. The core and alkane chains of the molecule were clearly imaged. It was found that the STM image contrast varied with bias voltage, especially in the core part.

* Authors to whom correspondence should be addressed. Tel.: 765-496-2699. E-mail: zw@ecn.purdue.edu; clbai@infoc3.icas.ac.cn.
† Institute of Chemistry, Chinese Academy of Sciences.
‡ University of Science and Technology of China.
§ School of Chemical Engineering, Purdue University.
‖ School of Materials Engineering, Purdue University.

10.1021/jp034396n CCC: $25.00
Published on Web 11/07/2003

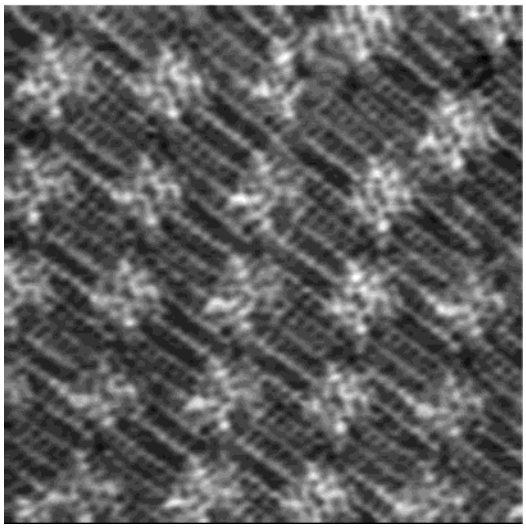

Figure 1. High-resolution STM image of $C_{14}O-Cu$ molecule acquired at bias of −700 mV; tunneling current, 415 pA; scan area, 12.51 × 12.51 nm.

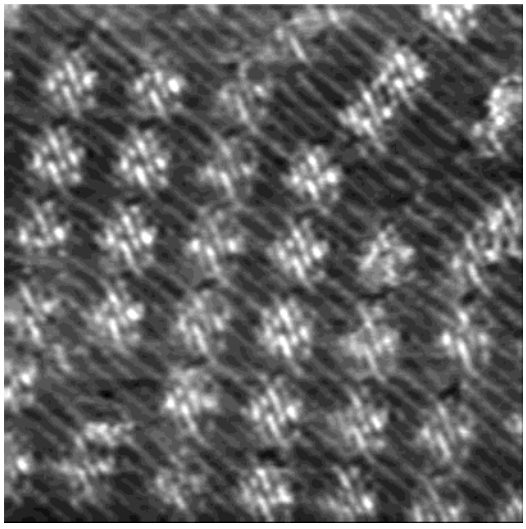

Figure 2. High-resolution STM image of $C_{14}O-Cu$ molecule acquired at bias of −800 mV; tunneling current, 415 pA; scan area, 16.92 × 16.92 nm.

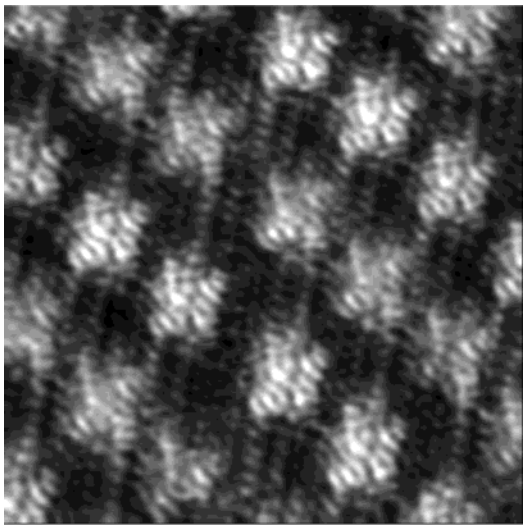

Figure 3. High-resolution STM image of $C_{14}O-Cu$ molecule acquired at bias of −830 mV, tunneling current, 415 pA; scan area, 12.30 × 12.30 nm.

Theoretical calculation was carried out to simulate the image variation. In the previous paper,[24] we have reported that STM image contrast of $C_{14}O-Cu$ molecules varied with tip−sample distance. These systematic studies will supply preliminary information for understanding the mechanism of STM image contrast.

Experiment

$C_{14}O-Cu$ containing covalently bonded alkanes was prepared and characterized according to the previous studies.[25,26]

The sample was dissolved in chloroform (HPLC grade, purchased from Aldrich Inc.) with a concentration of less than one percent. A droplet of the solution was deposited onto a freshly cleaved surface of HOPG (quality ZYB, Digital Instrument). The experiment was carried out in constant current mode using a Nanoscope IIIa SPM (Digital Instruments). STM tips were mechanically formed Pt/Ir (90%/10%) wire. All images presented in this paper were obtained with the same tip.

The theoretical simulation is based on the linear combination of atomic orbital-molecular orbital (LCAO-MO) method. The atomic orbits are represented by a double-numeric quality (DNP) basis set with polarization functions, which are comparable to Gaussian 6-31G** sets. In this work, the local density approximation (LDA) to the density functional theory (DFT) is employed with the Vosko-Wilk-Nusair parametrization of the local exchange-correlation energy.[27] The spin-restricted wave functions are utilized. The calculation is performed with the molecular simulation package DMOL.[28]

Results and Discussion

The submolecular features of $C_{14}O-Cu$, together with interdigitated alkanes, were well resolved at different tunneling conditions. $C_{14}O-Cu$ shows an appreciable bias-dependence effect in the STM imaging. With different bias voltage the image features in the core parts of the molecules are completely different, although the appearances of alkane chains are almost the same.

The image shown in Figure 1 was acquired at the bias of −700 mV. The core of a $C_{14}O-Cu$ molecule consists of many bright spots, and these spots are continuous in sight. There is a hole in the center of the core. This observation clearly indicates that the contributions from the molecular cores dominate the overall contrast. The zigzag lines interconnecting the bright regions correspond to the alkyl chains. Detailed examination of the STM image reveals that the alkyl chains of the adjacent molecules interdigitate, as expected for the crystalline phase.

The image in Figure 2, acquired at the bias of −800 mV, is different from that in Figure 1. The cores of $C_{14}O-Cu$ appear as a group of eight bright lobes, with an apparent central depression inside. The alkyl chains interdigitate and can be clearly resolved.

The image in Figure 3 was acquired at the bias of −830 mV. The cores of the molecules consist of four cover-like or ring-like structures, which are very compact. The cores are different from those of Figure 1 and Figure 2.

The above three images were acquired at the same tunneling current of 415 pA. The voltage-dependent STM images were obtained not only in the negative bias range, but also in the positive bias range. Figure 4 and Figure 5 were, respectively, acquired at the bias of 650 mV and 750 mV, although at the same tunneling current of 226.4 pA.

To ensure that the images are free from artifacts caused by the STM tip or the sample, we have repeated the experiment

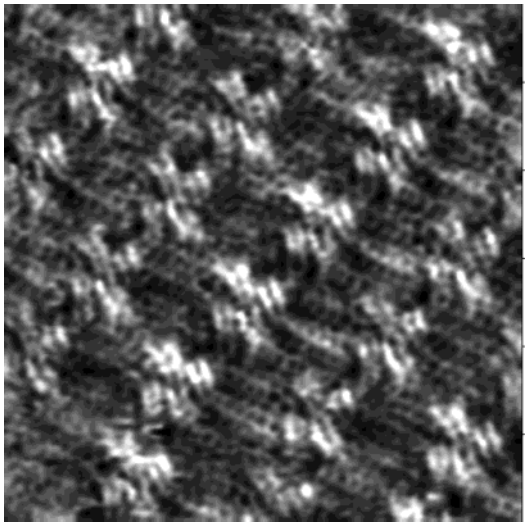

Figure 4. High-resolution STM image of $C_{14}O-Cu$ molecule acquired at bias of 650 mV; tunneling current, 226.4 pA; 14.75 × 14.75 nm.

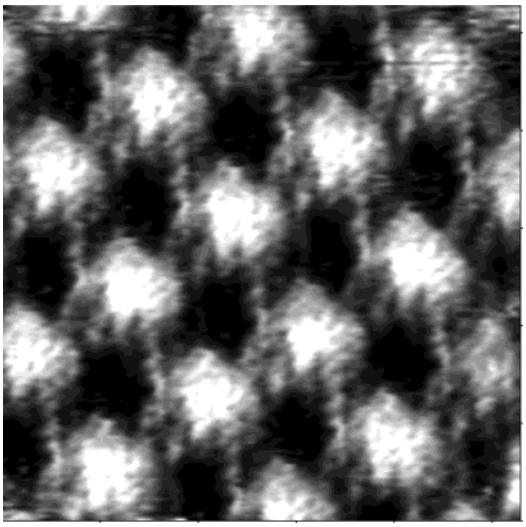

Figure 5. High-resolution STM image of $C_{14}O-Cu$ molecule acquired at bias of 750 mV; tunneling current, 226.4 pA; 13.23 × 13.23 nm.

with different tips to check the reproducibility. The contrast variation in STM images by altering bias was reproducible. For imaging of adsorbates with STM, the microscopy in fact probes the adsorbate and the substrate, both perturbed by their mutual interaction. Depending on the system, the direct contribution of the electronic states of the adsorbate is more or less strong. In the case of metal surfaces, where the interaction between adsorbate and substrate is usually strong, the general case is that the contribution of metal substrate to the tunnel current is decreased in the region of the adsorbate, i.e., creates a depression. But this is not the case for chemically inert graphite since the interaction is weaker. The direction contribution of the adsorbate to current is a bump, so physisorbed molecular monolayers on graphite provide an opportunity to image the molecules with a minimum of substrate perturbation.[15,17] This provides a direct approach to study the molecular orbital properties and its polarizability, which is a prerequisite for the understanding of the origin of STM contrast. In addition, alkylating the object molecules with suitable alkyl substituents was employed as molecule anchors to facilitate the immobilization of the molecules on graphite. The feature of the aliphatic chain makes it readily differentiated from other parts of the molecules, such as aromatic rings, hybrid, and halogen-atom-containing groups in the STM images.[29−31] Moreover, the aliphatic chain has little disruption to the electronic properties of the object molecules.[10] The HOPG surface used here will be a suitable substrate to investigate the $C_{14}O-Cu$ molecule. The observations described above clearly indicate that the contributions from the molecular cores dominate image contrast. The direct contribution to the STM image is dominantly from the electronic states of the $C_{14}O-Cu$ molecule.

In most cases, a large number of molecular orbitals (MO's) of the adsorbate above and below the Fermi level need to be included in order to accurately describe the tunnel current. The contribution of a given MO can be understood in terms of its energetic distance with the Fermi level, and the strength of its interactions with surface and tip. Moreover, these contributions from MO's can strongly interfere with each other, which can have a large influence on the contrast. Molecular orbitals of the adsorbate at an energy level different from the Fermi level participate via tails of resonance (or in other words, orbital mixing) in that "tunneling" state.[1,2,4,32−38]

To understand the origin of the image contrast variation, a theoretical simulation was performed on a C_1O-Cu molecule. Tersoff and Hamann's formula and its extension were adopted to simulate STM images.[1,39] By this method, the tunneling current in the STM can be expressed as

$$I(V) \propto \int_{E_F}^{E_F+eV} \rho(\vec{r},E)\, \mathrm{d}E \tag{1}$$

$$\rho(\vec{r},E) = \sum_i |\psi_i(\vec{r})|^2\, \delta(E - E_i) \tag{2}$$

where, $\rho(\vec{r},E)$, $\psi_i(\vec{r})$, E_F, and V are the local density of states (LDOS) of the sample, the sample wave function with energy E_i, the Fermi energy, and the sample bias voltage, respectively. Equations 1 and 2 allow us to obtain STM images only from the LDOS of the sample. The electronic structure of the C_1O-Cu molecule is calculated by using the density functional theory with the local density approximation within the DMOL package.[28] Four of the simulated STM images are shown in Figure 6 and Figure 7. Figure 6a involves the five molecular orbitals starting from the highest occupied molecular orbital (HOMO) which is partially occupied to the lowest unoccupied molecular orbital (LUMO) +3, while Figure 6b involves the seven molecular orbitals from HOMO to LUMO+5. They correspond to different LDOS. If the absolute value of bias in the experiment is increased, more molecular orbitals above or below the Fermi level have a contribution to the tunnel current. Therefore, STM can detect different LDOS and result in different images. Comparing Figures 6a and 6b with the $C_{14}O-Cu$ core regions in Figure 2 and Figure 3 respectively, the agreement between STM observation and theoretical simulation can be seen. Figure 7a involves the five occupied molecular orbitals from HOMO to HOMO-4, while Figure 7b involves seven occupied molecular orbitals from HOMO to HOMO-6. Comparing Figures 7a and 7b with the $C_{14}O-Cu$ core regions in Figure 4 and Figure 5, respectively, the agreement between STM observation and theoretical simulation can also be seen. The contrast variation with different bias voltage is attributed to the different LDOS. The bias difference between Figure 2 and Figure 3 is 30 mV, while the energy distance between LUMO+3 and LUMO+5 is 0.104 eV; the correlation coefficient between the LDOS and the STM images is 3.467. The bias difference between Figure 4 and Figure 5 is 100 mV, while the energy distance between HOMO-4 and HOMO-6 is 0.332 eV; the correlation coefficient between the LDOS and the STM images is 3.32, which

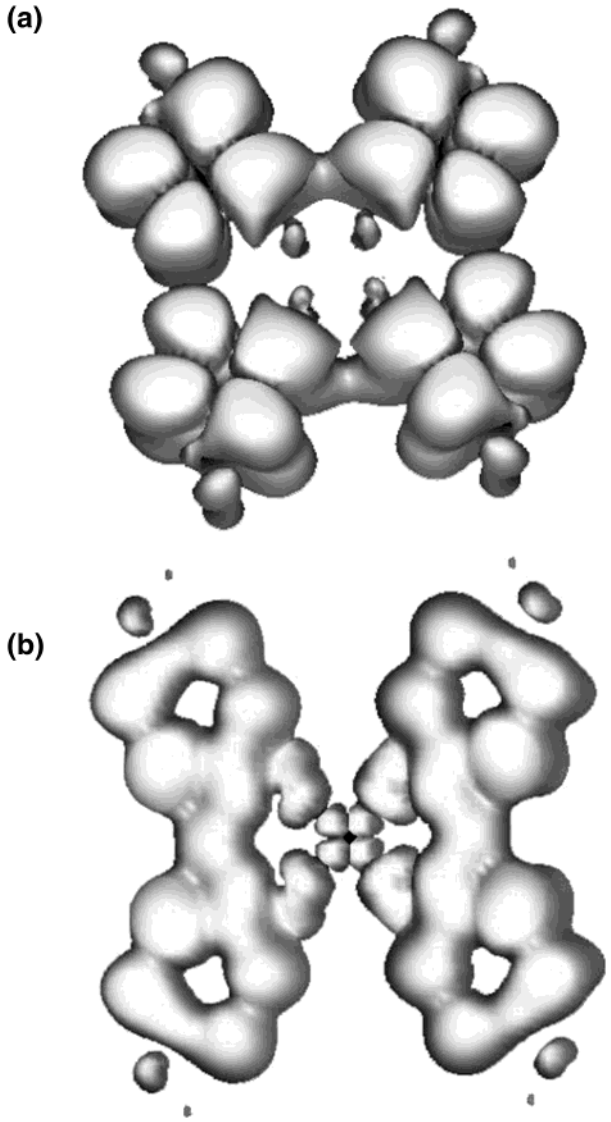

Figure 6. Local density of states of C_1O-Cu. (a) Corresponds to the core of $C_{14}O-Cu$ in Figure 2, and (b) to the core of $C_{14}O-Cu$ in Figure 3.

approximates the coefficient 3.467. This experiment clearly demonstrates that the bias-voltage dependence of the images originates from the effect of electronic structure. Particularly, in the research system, STM images changed with bias changes of 100 mV or less. Usually it is unlikely that such small bias changes result simply in the probing of different molecular orbitals. This may be attributed to the extremely sharp electronic resonances of this system.

Conclusion

The contrast variation of STM images of $C_{14}O-Cu$ molecules has been investigated on the HOPG surface. The molecular structure was clearly imaged. It was found that the image contrast of $C_{14}O-Cu$ molecules changed with bias. Particularly, STM images changed with bias changes of 100 mV or less. Theoretical simulation results were in agreement with STM observation.

Acknowledgment. The authors thank The National Nature Science Foundation of China (No. 20103008, 20073053) and the Foundation of the Chinese Academy of Sciences for their financial support.

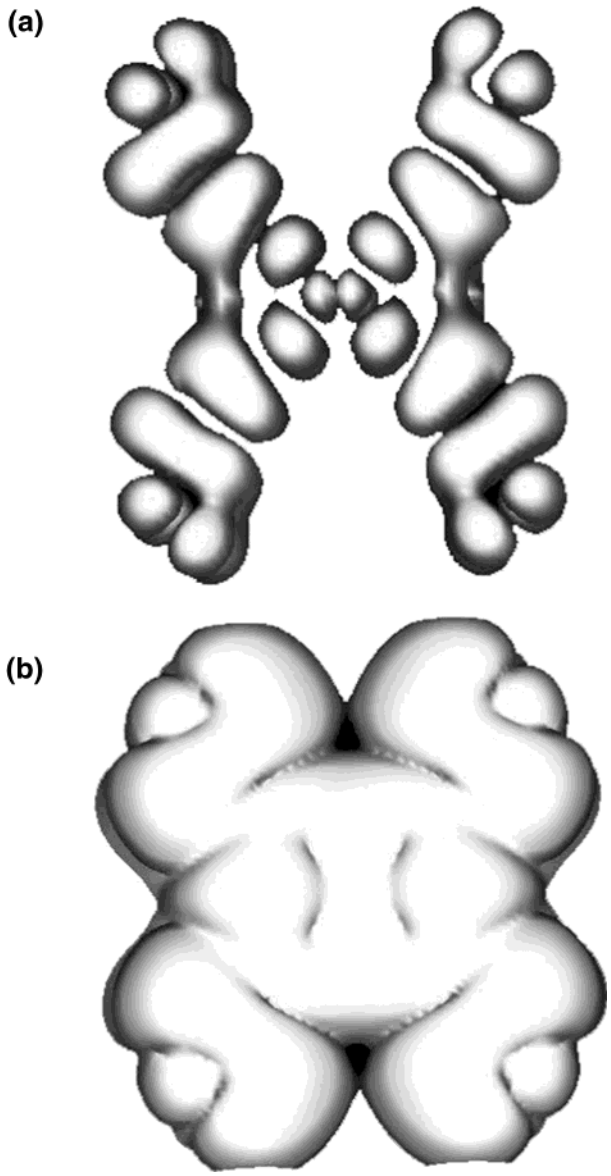

Figure 7. Local density of states of C_1O-Cu. (a) Corresponds to the core of $C_{14}O-Cu$ in Figure 4, and (b) to the core of $C_{14}O-Cu$ in Figure 5.

References and Notes

(1) Tersoff, J.; Hamann, D. R. *Phys. Rev. B* **1985**, *31*, 805.
(2) Bardeen, J. *Phys. Rev. Lett.* **1961**, *6*, 57.
(3) Lang, N. D.; Doyen, G. *Scanning Tunneling Microscopy III*, 2nd ed.; Wiesendanger, R., Güntherodt, H. J., Eds.; Springer-Verlag: Berlin, 1996.
(4) Padowitz, D. F.; Hamers, R. J. *J. Phys. Chem. B* **1998**, *102*, 8541.
(5) Sautet, P.; Joachim, C. *Chem. Phys. Lett.* **1991**, *185*, 23.
(6) Fisher, A. J.; Blöchl, D. E. *Phys. Rev. Lett.* **1993**, *70*, 3236.
(7) Sautet, P. *Chem. Rev.* **1997**, *97*, 1097.
(8) Bai, C. Scanning Tunneling Microscopy, 2nd revised ed.; Springer, Shanghai Scientific & Technical Publishers: New York, 2000.
(9) Sautet, P.; Joachim, C. *Surf. Sci.* **1992**, *271*, 387.
(10) Qiu, X. H.; Wang, C.; Zeng, Q. D.; Xu, B.; Yin, S. X.; Wang, H. N.; Xu, S. D.; Bai, C. L. *J. Am. Chem. Soc.* **2000**, *122*, 5550.
(11) Lang, N. D. *Phys. Rev. Lett.* **1987**, *58*, 45.
(12) Lang, N. D. *Phys. Rev. B* **1986**, *34*, 5947.
(13) Schimizu, T.; Tsukada, M. *Solid State Commun.* **1993**, *87*, 193.
(14) Schimizu, T.; Tsukada, M. *J. Vac. Sci. Technol. B* **1994**, *12*, 2200.
(15) Tsukada, M.; Kobayashi, K. *Appl. Surf. Sci.* **1993**, *67*, 235.
(16) Joachim, C.; Gimzewshi, J. K. *Europhys. Lett.* **1995**, *30*, 409.
(17) Smith, D. P. E.; Hörber, H.; Binnig, G. *Nature* **1990**, *344*, 641.
(18) Eichhorst-Gerner, K.; Stabel, A.; Moesser, G.; Declerq, D.; Valiyaveetti, S.; Enkelmann, V.; Mullen, K.; Rabe, J. P. *Angew. Chem., Int. Ed. Engl.* **1996**, *35*, 1492.

(19) Foster, J. S.; Frommer, J. E. *Nature* **1988**, *333*, 542.
(20) Spong, J. K.; Mizes, H. A.; Lacomb, L. J., Jr.; Dovek, M. M.; Frommer, J. E.; Foster, J. S. *Nature* **1989**, *338*, 137.
(21) Rabe, J. P.; Buchholz, S. *Science* **1991**, *53*, 424.
(22) Rabe, J. P.; Buchholz, S. *Phys. Rev. Lett.* **1991**, *66*, 2096.
(23) Cincotti, S.; Rabe, J. P. *Appl. Phys. Lett.* **1993**, *62*, 3531.
(24) Wang, Z. G.; Zeng, Q. D.; Wan, L. J.; Wang, C.; Yin, S. X.; Bai, C. L.; Wu, X. J.; Yang, J. L. *Surf. Sci. Lett.* **2002**, *513*, L436.
(25) Ohta, K.; Ishii, A.; Yamamoto, I.; Matsuzaki, K. *J. Chem. Soc., Chem. Commun.* **1984**, 1099.
(26) Ohta, K.; Ishii, A.; Muroki, H.; Yamamoto, I.; Matsuzaki, K. *Mol. Cryst. Liq. Cryst.* **1985**, *116*, 299.
(27) Vosko, S. H.; Wilk, L.; Nusair, M. *Can. J. Phys.* **1980**, *58*, 1200.
(28) DMOL Version 960, Density Functional Theory electronic structure program, Molecular Simulations Inc.: 1996.
(29) Lippel, P. H.; Wilson, R. J.; Miller, M. D.; Wöll, Ch.; Chiang, S. *Phys. Rev. Lett.* **1989**, *62*, 171.
(30) Lu, X.; Hipps, K. W. *J. Phys. Chem. B* **1997**, *101*, 5391.
(31) Chiang, S. *Chem. Rev.* **1997**, *97*, 1083.
(32) Yu, E. T. *Chem. Rev.* **1997**, *97*, 1017.
(33) Chavy, C.; Joachim, C.; Altibell, A. *Chem. Phys. Lett.* **1993**, *214*, 569.
(34) Giancarlo, L. C.; Flynn, G. W. *Annu. Rev. Phys. Chem.* **1998**, *49*, 297.
(35) Kenkre, V. M.; Biscarini, F.; Bustamante, C. *Ultramicroscopy* **1992**, *42*, 122.
(36) Ness, H.; Fish, A. J. *Phys. Rev. B* **1997**, *55*, 10081.
(37) Ness, H.; Fish, A. J. *Phys. Rev. B* **1997**, *56*, 12469.
(38) Faglioni, F.; Claypool, C. L.; Lewis, N. S.; Goddard, W. A., III. *J. Phys. Chem. B* **1997**, *101*, 5996.
(39) Tersoff, J.; Hamann, D. R. *Phys. Rev. Lett.* **1983**, *50*, 1998.